



Comparing observed and modelled components of the Atlantic Meridional Overturning Circulation at 26° N

Harry Bryden¹, Jordi Beunk², Sybren Drijfhout^{1,3}, Wilco Hazeleger², and Jennifer Mecking⁴

¹School of Ocean and Earth Science, University of Southampton, Southampton, UK

²Department of Earth Sciences, University of Utrecht, Utrecht, the Netherlands

³Department of Physics, University of Utrecht, Utrecht, the Netherlands

⁴National Oceanography Centre, Southampton, UK

Correspondence: Harry Bryden (h1b@soton.ac.uk)

Received: 14 November 2023 – Discussion started: 16 November 2023

Revised: 5 February 2024 – Accepted: 21 February 2024 – Published: 17 April 2024

Abstract. The Coupled Model Intercomparison Project (CMIP) allows the assessment of the representation of the Atlantic Meridional Overturning Circulation (AMOC) in climate models. While CMIP Phase 6 models display a large spread in AMOC strength, the multi-model mean strength agrees reasonably well with observed estimates from RAPID¹, but this does not hold for the AMOC's various components. In CMIP Phase 6 (CMIP6), the present-day AMOC is characterized by a lack of lower North Atlantic Deep Water (INADW) due to the small scale of Greenland–Iceland–Scotland Ridge overflow and too much mixing. This is compensated for by increased recirculation in the subtropical gyre and more Antarctic Bottom Water (AABW). Deep-water circulation is dominated by a distinct deep western boundary current (DWBC) with minor interior recirculation compared with observations. The future decline in the AMOC of 7 Sv by 2100 under a Shared Socioeconomic Pathway 5-8.5 (SSP5-8.5) emission scenario is associated with decreased northward western boundary current transport in combination with reduced southward flow of upper North Atlantic Deep Water (uNADW). In CMIP6, wind stress curl decreases with time by 14 % so that wind-driven thermocline recirculation in the subtropical gyre is reduced by 4 Sv (17 %) by 2100. The reduction in western boundary current transport of 11 Sv is more than the decrease in wind-driven gyre transport, indicating a decrease over time in the component of the Gulf Stream originating from the South Atlantic.

1 Introduction

The Atlantic Meridional Overturning Circulation (AMOC) is the Atlantic part of the global overturning circulation. The global overturning circulation, in which deep waters formed at high latitudes in the northern Atlantic and Weddell Sea flow equatorward, upwell, circulate and eventually flow as upper waters back towards the formation regions, transports heat, fresh water, nutrients and CO₂ throughout the global ocean. The AMOC includes North Atlantic Deep Water (NADW) formation in the subpolar and polar regions of the northern Atlantic, southward flow of NADW in deep western boundary currents, wind-driven circulation in the subtropical and subpolar gyres, and northward flow of upper waters (notably in the Gulf Stream). Upwelling of NADW occurs principally outside of the North Atlantic. Our understanding of the strength, variability and structure of the AMOC has improved since the deployment of the RAPID¹ array, which has monitored the AMOC volume transport at 26° N since April 2004 (Moat et al., 2020). Additionally, these observations serve as invaluable reference data for the representation of the AMOC in coupled climate and Earth system models. The most recent phase of the Coupled Model Intercomparison Project, CMIP Phase 6, allows us to assess the representation of the AMOC in these models. The models project AMOC strength will decline over the next century (Lee et al., 2021). Here, we compare observed and modelled

¹RAPID is used here as shorthand for the RAPID-Meridional Overturning Circulation and Heatflux Array-Western Boundary Time Series at 26° N (Moat et al., 2022).

components of the AMOC over the historical period 2004–2014 and then assess how the ensemble mean of the CMIP Phase 6 (CMIP6) transport components changes in a declining AMOC over the next century under a Shared Socioeconomic Pathway 5-8.5 (SSP5-8.5) emission scenario.

The RAPID AMOC observations from 2004–2018 indicate that the AMOC has declined by 2.4 Sv, about 12 %, from 18.3 to 15.9 Sv (Bryden, 2021). The decline is primarily evident in the reduced southward transport of lower North Atlantic Deep Water (INADW), which is balanced by slightly reduced Gulf Stream transport and more southward recirculation within the subtropical gyre. In CMIP6 models, the AMOC is projected to decline by about 40 % over the 21st century (Weijer et al., 2020). Here, we analyse 19 CMIP6 model projections in order to identify which components bring about the AMOC decline, seeking insights into how the AMOC may change within the continuing RAPID observational framework.

The Coupled Model Intercomparison Project (CMIP) is a comprehensive effort of modelling centres around the world to improve our understanding of past, present and future changes in the climate system (Eyring et al., 2016; O'Neill et al., 2016). Even though CMIP6 shows improvements compared to previous CMIP generations, model biases related to the AMOC persist. These include a shallow bias towards the deep cell, too much deep convection, and an inadequate temperature difference between the AMOC's upper and lower limbs. Additionally, CMIP6 models largely underestimate low-frequency variability in the AMOC and show large inter-model differences in their AMOC representation (Weijer et al., 2020).

The RAPID array has monitored the AMOC volume transport at 26° N since April 2004 (Smeed et al., 2018). The transport through the cross section is estimated by the decomposition of the AMOC into three components: (1) transport through the Florida Straits, (2) Ekman surface transport generated by zonal wind stress and (3) density-driven interior transport estimated from mooring measurements. Mid-ocean interior transport is further broken down into thermocline recirculation (0–800 m depth), Intermediate Water transport (800–1100 m), upper North Atlantic Deep Water (1100–3000 m) and lower North Atlantic Deep Water (3000–5000 m). The goal of this study is to gain insight into the cause of disagreement between CMIP6 models and RAPID data in terms of AMOC strength, structure and variability. We decompose the modelled AMOC transport at 26° N from CMIP6 into the same transport components as those measured by the RAPID array. We compare the CMIP6 transport components with the observed RAPID components for the historical period 2004–2014. We then examine the change in these components of CMIP6 under the SSP5-8.5 emission scenario from the historical period until 2100.

2 Data and methods

Monthly averages of AMOC estimates from the RAPID array are compared to the historical simulations of the 19 CMIP6 models. Note that only the overlapping period (April 2004–December 2014) was investigated. Details of the 19 CMIP6 models are given in Table 1. The SSP5-8.5 future projection for 2015–2100 is then used to investigate how the AMOC may change in future projections. For each model, one ensemble member was used, as defined in Table 1.

A cross section between Florida and the African continent at the latitude closest to 26° N was selected for each model. The net transport through the section, approximately -1 Sv for each model due to the Bering Strait throughflow, was removed before computing the AMOC components from the meridional velocities as follows.

With regard to the Florida Straits (FS) transport, CMIP6 models do not properly resolve the Bahama islands, and, as a result, they do not resolve the Florida Straits either. For this reason, the following definition is used. The boundary between the Florida Straits (FS) transport and mid-ocean transport is defined as the longitude where the depth-averaged transport (from the surface down to the depth of maximum overturning) changes from positive (northward) to negative (southward). This definition thus identifies the FS transport as the western boundary current, thereby including the transport by the Antilles Current, which in CMIP6 models cannot be separated from the Florida Current.

For each model, we have established the following criteria to define thermocline recirculation, upper North Atlantic Deep Water, lower North Atlantic Deep Water and Antarctic Bottom Water. The decision was to use potential temperature to determine the boundaries between upper and lower North Atlantic Deep Water in the CMIP6 models. This choice was motivated by the indistinct upper boundary (in terms of depth) of lower North Atlantic Deep Water in the models.

- Thermocline recirculation (tr) is east of the FS and extends from the surface down to the depth where the horizontally averaged potential temperature is 8 °C.
- Intermediate Water (iw) is east of the FS and between the depth where the horizontally averaged potential temperature is 8 °C and the depth of maximum overturning.
- Upper North Atlantic Deep Water (uNADW) is between the depth of maximum overturning and the depth where the horizontally averaged potential temperature is 3 °C.
- Lower North Atlantic Deep Water (INADW) is between the depth where the horizontally averaged potential temperature is 3 °C and the depth where the horizontally averaged transport changes from negative to positive.

Table 1. Metadata and references for the models analysed in this study. The choice of models is motivated by the fact that historical and SSP5-8.5 data are available for all variables used, including meridional velocity, zonal wind stress, salinity and temperature. In addition, only models that use horizontal depth values are included. The choice of ensemble member is indicated, and the preferred ensemble member comprises realization 1, initialization 1, physics 1 and forcing 1, indicated by “r1i1p1f1”. For some models, forcing 1 was not available, so a different ensemble member was chosen, making sure that the forcing version (v6.2.0) was the same. References are from the Earth System Grid Federation.

Model	Modelling centre	Horizontal resolution (°)	Variant label	Data reference (historical)	Data reference (SSP5-8.5)
CAMS-CSM1-0	CAMS	1 × 1	r1i1p1f1	Rong (2019a)	Rong (2019b)
CAS-ESM2-0	CAS	1 × 1	r1i1p1f1	Chai (2020)	Unknown (2018)
CESM2-WACCM	NCAR	1 × 1	r1i1p1f1	Danabasoglu (2019b)	Danabasoglu (2019a)
CIESM	THU	1 × 1	r1i1p1f1	Huang (2019)	Huang (2020)
CMCC-CM2-SR5	CMCC	1 × 1	r1i1p1f1	Lovato and Peano (2020a)	Lovato and Peano (2020b)
CMCC-ESM2	CMCC	1 × 1	r1i1p1f1	Lovato et al. (2021a)	Lovato et al. (2021b)
CNRM-CM6-1	CNRM-CERFACS	1 × 1	r1i1p1f2	Voltaire (2019a)	Voltaire (2019b)
CNRM-ESM2-1	CNRM-CERFACS	1 × 1	r2i1p1f2	Seferian (2018)	–
CanESM5	CCCma	1 × 1	r1i1p1f1	Swart et al. (2019a)	Swart et al. (2019b)
EC-Earth3	EC-Earth Consortium	1 × 1	r1i1p1f1	EC-Earth Consortium (2021)	EC-Earth Consortium (2019)
FIO-ESM-2-0	FIO-QLNM	1 × 1	r1i1p1f1	Song et al. (2019a)	Song et al. (2019b)
HadGEM3-GC31-LL	MOHC	1 × 1	r1i1p1f3	Ridley et al. (2019a)	Good (2020)
HadGEM3-GC31-MM	MOHC	0.25 × 0.25	r1i1p1f3	Ridley et al. (2019b)	Good et al. (2019)
IPSL-CM6A-LR	IPSL	1 × 1	r1i1p1f1	Boucher et al. (2021)	Boucher et al. (2019)
MPI-ESM1-2-HR	MPI	0.4 × 0.4	r1i1p1f1	Jungclaus et al. (2019)	Schupfner et al. (2019)
MPI-ESM1-2-LR	MPI	1.5 × 1.5	r1i1p1f1	Wieners et al. (2019a)	Wieners et al. (2019b)
MRI-ESM2-0	MRI	1 × 0.5	r1i1p1f1	Yukimoto et al. (2019a)	Yukimoto et al. (2019b)
NESM3	NUIST	1 × 1	r1i1p1f1	Cao and Wang (2019)	Cao (2019)
UKESM1-0-LL	MOHC	1 × 1	r1i1p1f2	Tang et al. (2019)	Good et al. (2019)

- Antarctic Bottom Water (AABW) is between the depth where horizontally averaged transport changes from negative to positive and the bottom.
- Ekman (ek) refers to near-surface ageostrophic transport estimated from the zonal wind stress.
- The multi-model mean (MMM) of the 19 models for each component is then calculated along with the standard deviation.

3 Results

Figure 1 compares the RAPID observations of the AMOC transport components with the simulations of the CMIP6 components for the historical period 2004–2014. For this historical period (2004–2014), the CMIP6 MMM of the AMOC underestimates the observed AMOC transport by 2.2 Sv (Table 2). The underestimation of AMOC strength in the CMIP6 models is likely related to the reduced transport of INADW, which is due to the small scale of Greenland–Iceland–Scotland Ridge overflow compared to the resolution of the models and excessive mixing at this location. In a study of deep waters in CMIP6, Heuzé (2021) noted that the models did form water masses with similar properties to those in INADW in the Nordic Seas, but none of the deep waters made it over the ridge and into the Iceland or Irminger basins. In the models, this lack of INADW is partially compensated for by an increased southward flow of uNADW, so

the total southward flow of deep water in CMIP6 is comparable to that observed by RAPID. The variability in NADW is underestimated, most likely due to the inability of models to reproduce INADW overflow. Deep-water circulation in models is dominated by a distinct DWBC with minor interior recirculation compared with observations. The CMIP6 MMM Florida Straits (FS) transport (37.4 Sv) is larger than the observed Florida Straits transport (31.3 Sv). The relatively coarse-resolution models do not resolve the narrow Florida Straits, and the modelled western boundary current includes the narrow Antilles Current east of The Bahamas as well as the Gulf Stream flow through the Florida Straits. The Antilles Current has a maximum northward velocity at 360 m depth, and the core of the current is within 50 km of the Bahama islands. Recent estimates of the Antilles Current transport are about 5 Sv (Meinen et al., 2019), and adding this transport to the observed Florida Straits transport suggests that the observed (36.3 Sv) and modelled (37.4 Sv) western boundary current transports are similar. The low-frequency variability in the Florida Straits transport is largely overestimated in CMIP6 models, and we hypothesize that the inclusion of the Antilles Current in this component in the models may be a significant contributor to this variability, as the observed Antilles Current transport exhibits an rms variability of 7.5 Sv that is not correlated with Florida Straits transport variability. The MMM thermocline recirculation (τ) in CMIP6 models (−26.2 Sv) is larger than that observed by the RAPID array (−18.6 Sv), though, again, this may be due to issues concerning how the Antilles Current transport is accounted for in the observations and in the models. RAPID

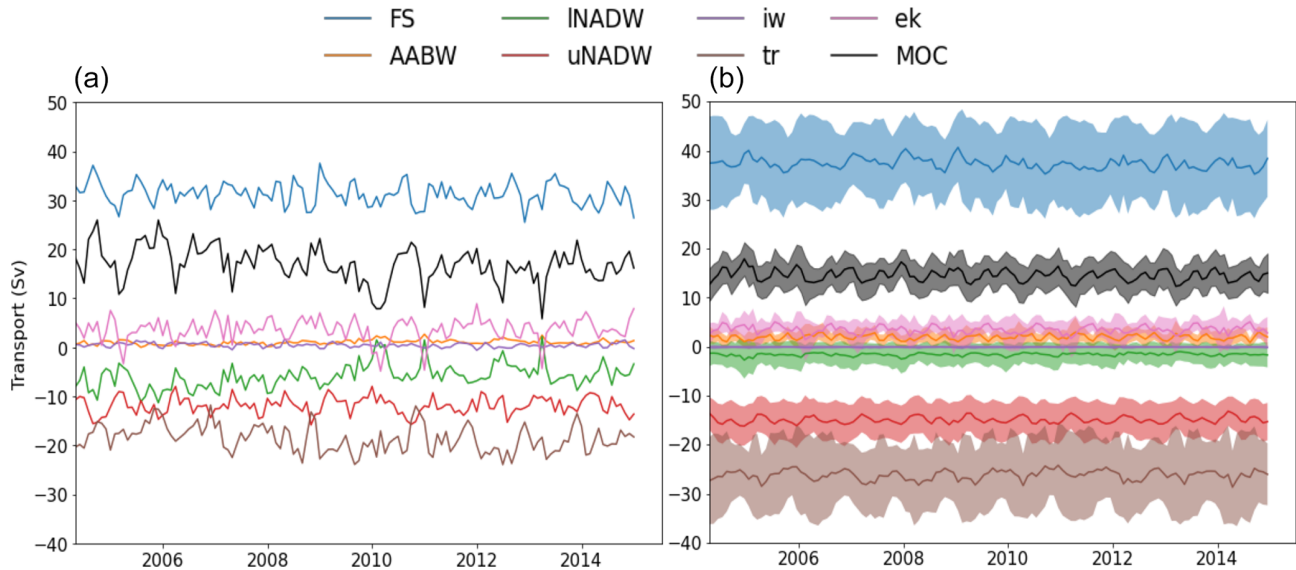


Figure 1. Historical time series for (a) RAPID data and (b) multi-model mean CMIP6 data. Shaded areas each indicate 1 standard deviation of the ensemble spread. Note that MOC stands for Meridional Overturning Circulation.

estimates thermocline recirculation to be the overall southward flow above 800 m depth between The Bahamas and Africa, and this overall flow includes both the Antilles Current transport and the mid-ocean thermocline recirculation associated with the wind-driven subtropical gyre. If we separate out the northward Antilles Current transport of 5 Sv, then the mid-ocean thermocline recirculation in RAPID would be -23.6 Sv (Table 2), which is in more reasonable agreement with the CMIP6 MMM thermocline circulation of -26.2 Sv. Overall, the MMM circulation in CMIP6 models for the historical period reasonably represents the observed circulation in RAPID with the exception of the underestimated INADW transport associated with issues of model representation of flows over ridges.

CMIP6 model projections suggest that the AMOC will decline over the next century, as noted by Weijer et al. (2020). Here, we find that the AMOC declines by 45 % over the period 2015–2100 in the MMM of the 19 CMIP6 projections. For comparison, over the RAPID time period 2004–2021, the AMOC exhibited a small reduction (on the order of 12 %) that is manifested principally in reduced southward transport of INADW (Bryden, 2021). It is of interest to identify which components contribute to the projected 45 % decline in the AMOC over the coming century in CMIP6 simulations.

All 19 CMIP6 models analysed here project a decline in the AMOC over the 21st century (Table 3). This decline in the AMOC under the SSP5-8.5 emission scenario is in line with other modelling studies (Levang and Schmitt, 2020; Weijer et al., 2020; Roberts et al., 2020). Averaged over the 19 models, the AMOC declines from 2004–2014 to 2090–2100 by 6.6 Sv (or 45 %) when considering the AMOC transport for the historical period (Fig. 2). We find that the decline

in the AMOC at 26° N in CMIP6 models from 2015–2100 is dominated by a 30 % decrease in western boundary current transport (FS in Fig. 2) and a 34 % reduction in southward deep-water transport (uNADW in Fig. 2). As Ekman (ek) transport shows no significant change in the model projections, the AMOC decline of 6.6 Sv in the upper waters is the result of the difference between the decline in western boundary current (FS) transport of 11.0 Sv and the 17 % decline in southward thermocline recirculation (tr) of 4.4 Sv. For the lower waters, the overall decline in northward transport of upper waters of 6.6 Sv is compensated for by a decrease in uNADW transport of 6.4 Sv and a small increase in northward AABW transport of 0.2 Sv, meaning that the net transport through the cross section remains zero.

To examine changes in wind-driven circulation over the 21st century in the subtropical North Atlantic, we examined the mean wind stress curl at the 26° N section for the historical and SSP5-8.5 periods. The values are negative (i.e. rotation is clockwise), which results in southward mid-ocean Sverdrup transport. Since the upper-level gyre circulation is driven by wind stress curl (DiNezio et al., 2009; Zhao and Johns, 2014), we expect a decrease in this driver to affect both the Florida Straits transport and thermocline recirculation. Averaged over the model projections, wind stress curl decreases from about $6 \times 10^{-8} \text{ m s}^{-2}$ by 14 %. On the basis of Sverdrup dynamics, we expect this change in wind stress curl will reduce thermocline recirculation at 26° N, and indeed thermocline recirculation does decrease by 4.4 Sv (or 17 %) over the 21st century. We conclude that the reduction in thermocline recirculation is almost entirely caused by a decline in wind stress curl, and the decline in the directly wind-driven component of the AMOC is exactly reflected in

Table 2. Components of the Atlantic Meridional Overturning Circulation at 26° N. The modelled western boundary current includes both the Florida Straits and Antilles Current transports. The observed Antilles Current (AC) transport of 5 Sv is a rounded value derived from the mean transport of 4.7 ± 7.5 Sv, given by Meinen et al. (2019). For standard RAPID analyses, thermocline recirculation includes the Antilles Current transport.

	CMIP6 average			
	RAPID (2004–2014)	Historical (2004–2014)	2090–2100	Decline
Upper water				
Florida Straits (FS)	31.3	37.4	26.4	11 (30 %)
Ekman (ek)	3.6	3.5	3.4	0.1 (1 %)
Intermediate Water	0.4	–	–	
Thermocline recirculation (tr)	–18.6			
AMOC = FS + ek + iw + tr	16.7			
Upper water				
Antilles Current (AC)	5			
Western boundary current (FS + AC)	36.3	37.4	26.4	11 (30 %)
Thermocline recirculation (tr) – AC	–23.6			
Modelled thermocline recirculation		–26.2	–21.8	4.4 (17 %)
AMOC = FS + ek + iw + Model tr		14.7	8.0	6.7 (45 %)
Deep water				
uNADW	–11.9	–14.9	–9.9	5.0 (34 %)
INADW	–5.9	–1.6	–0.2	1.4 (85 %)
AABW	1.0	1.9	2.1	–0.2 (9 %)
AMOC = uNADW + INADW + AABW	–16.8	–14.6	–8.0	6.6 (45 %)

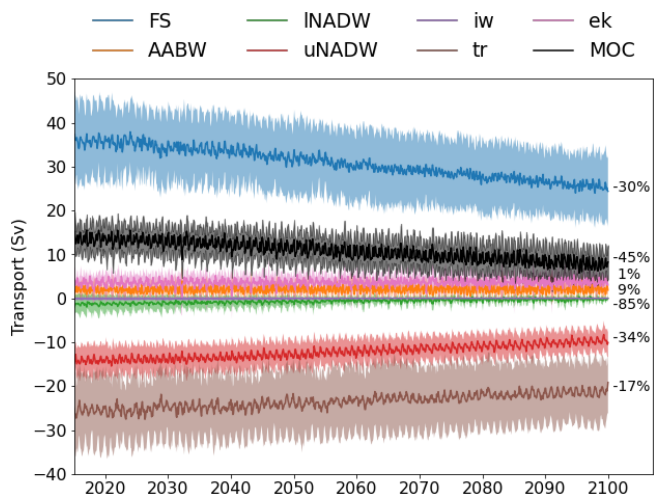


Figure 2. Multi-model mean time series for each component under the SSP5-8.5 emission scenario. Shaded areas each illustrate 1 standard deviation of the inter-model spread. Percentages show the decline relative to the historical period.

the 17 % decline in thermocline recirculation (tr in Fig. 2). On the basis of the theory of western intensification (Stommel, 1948), the decrease in wind stress curl should also lead to a decrease in western boundary current transport by a similar amount. Thus, we can explain the decrease in western

boundary current transport of 4.4 Sv over the 21st century as being due to changes in the wind forcing.

The change in western boundary current transport of 11 Sv in the CMIP6 projections is due to a reduction in the wind-driven component of 4.4 Sv and to a reduction in the component of the Gulf Stream flow originating from the South Atlantic of 6.6 Sv. The overall 6.6 Sv reduction in the northward flow of the upper waters is then compensated by a reduction in the southward flow of the deep waters. In CMIP6, the reduction in the southward flow of deep water is almost entirely due to the decreased DWBC transport of uNADW over the period 2015–2100. Hence, the decline in the thermohaline component is reflected in the 34 % decline in uNADW transport (uNADW in Fig. 2). Overall, the projected AMOC reduction in CMIP6 over the 21st century is due to a reduction in the thermohaline circulation, where there is less northward transport of upper waters primarily by the western boundary current and less southward deep-water transport by the deep western boundary current.

4 Discussion

There is much interest in whether the AMOC will decline over the 21st century. Recent analyses of historical observations using Bayesian methods have concluded that the Gulf Stream has weakened by about 1 Sv over the past 40 years

Table 3. Values of the total AMOC for each model. Shown are the historical mean values, 2090–2100 mean values, absolute change and relative change. Changes are relative to the historical period.

Model name	Historical mean (Sv)	2090–2100 mean (Sv)	Change (Sv)	Change (%)
CAMS-CSM1-0	12.4	8.9	−3.5	−28
CAS-ESM2-0	18.4	13.7	−4.7	−26
CESM2-WACCM	17.9	6.8	−11.1	−62
CIesm	11.4	4	−7.4	−65
CMCC-CM2-SR5	14.2	9.2	−5.0	−35
CMCC-ESM2	13.3	9.3	−4.0	−30
CNRM-CM6-1	15.7	6.9	−8.8	−56
CNRM-ESM2-1	15.3			
CanESM5	11.4	5.5	−5.9	−52
EC-Earth3	16.2	10.7	−5.5	−34
FIO-ESM-2-0	17.7	10.7	−7.0	−39
HadGEM3-GC31-LL	15.2	7.9	−7.3	−48
HadGEM3-GC31-MM	15.4	6.5	−8.9	−58
IPSL-CM6A-LR	11.6	6.5	−5.1	−44
MPI-ESM1-2-HR	14.8	8.6	−6.2	−42
MPI-ESM1-2-LR	16.6	11.4	−5.2	−31
MRI-ESM2-0	15.4	5	−10.4	−67
NESM3	9.0	5	−4.0	−45
UKESM1-0-LL	15.6	7.8	−7.8	−50

(Piecuch and Beal, 2023) and that the AMOC will decline markedly over the next 50 years (Ditlevsen and Ditlevsen, 2023). These studies have generated great media interest. Here, we use CMIP6 forward model projections under expected climate forcing (SSP5-8.5) to assess what state-of-the-art coupled climate models “predict” for the AMOC over the 21st century. McCarthy and Caesar (2023) have argued that models like CMIP6 have not been able to simulate large AMOC variations in the paleo record and hence should not be relied upon to generate accurate projections of future AMOC. Comparisons between model projections and observed circulation variability, like those presented above, do provide an assessment of the models’ ability to reliably project the future course of the AMOC. CMIP6 models project declines in both the wind-driven and thermohaline components of the AMOC out to 2100. Comparing these projections with ongoing observations, like those from RAPID, then provides a reality check on the ability of present models to define future climate change.

Over the SSP5-8.5 period (2015–2100) in CMIP6 projections, we find declines in western boundary current transport, thermocline recirculation and NADW transport. Decreased thermocline recirculation is related to a decline in wind stress curl, and this decline is also expected to contribute to the decline in Gulf Stream transport. However, the decline in western boundary current transport in CMIP6 models is substantially greater than the decline in wind stress curl and accompanying thermocline recirculation. Therefore, for the upper-water circulation, the CMIP6-projected decline in the AMOC is mostly caused by a decrease in the component of the west-

ern boundary current associated with the thermohaline circulation. For the lower-water circulation, the decline in southward transport over the SSP5-8.5 period is associated with reduced uNADW transport. The overall reduction in southward deep-water transport suggests a decline in NADW formation.

In a similar study, Asbjørnsen and Arthun (2023) examined future changes in the AMOC using 14 CMIP6 models and found the AMOC weakened by 8.5 Sv over the coming century. Using their ensemble, the Gulf Stream weakened by 33 % (or 11.2 Sv), 3.7 Sv of which was due to change in wind stress, and the deep western boundary current transport weakened by 8.5 Sv. As noted above, the CMIP6 projections are consistent in projecting a decline in the AMOC this century (Table 3), but the exact extent of the AMOC reduction depends on which models are used for the study.

Because the AMOC is responsible for most of the northward heat transport in the Atlantic Ocean (Johns et al., 2011, 2023), CMIP6 model projections also exhibit a decrease in the northward heat transport at 26° N over the 2015–2100 time period (Mecking and Drijfhout, 2023). The northward ocean heat transport in the Atlantic Ocean across 26° N decreases by an average of 0.3 PW under the SSP5-8.5 emission scenario, and this represents a 30 % decline from the historical value of 1.0 PW.

The decline in the thermohaline circulation at 26° N implies that the overturning circulation south of 26° N – that is, in the global circulation outside the North Atlantic – has also changed. The extra-Atlantic circulation converts deep water into upper and intermediate waters so that the south-

ward deep-water flow across 26° N and out of the North Atlantic must ultimately be converted within the global ocean into upper and intermediate waters that flow back into the North Atlantic and northward across 26° N. The decline in the North Atlantic thermohaline circulation at 26° N suggests that this global-scale overturning circulation must also have changed. Baker et al. (2023) have explored how two mechanisms converting deep water into upper water south of 26° N change within CMIP6 simulations. The two mechanisms considered are Southern Ocean upwelling, associated with eastward wind stress around Antarctica (Toggweiler and Samuels, 1993), and Indo-Pacific diffusive upwelling, associated with deep interior mixing (Munk, 1966). Baker et al. found that the wind stress around Antarctica did not decline enough to account for a reduced 6 Sv upwelling of deep water; in fact, there appeared to be a small increase in Southern Ocean wind stress and upwelling. Instead, they found evidence in the CMIP6 projections that the interior Indo-Pacific upwelling declined enough to account for the reduced conversion of deep waters into thermocline waters. They attributed such decline to global warming, which increases stratification (Li et al., 2020) and inhibits vertical mixing and associated upwelling.

Overall, the Atlantic and global overturning circulations appear to decline in CMIP6 projections for 2015–2100. The manifestation of these declines at 26° N include a reduction in the southward transport of NADW and a compensating reduction in the northward flow of upper and thermocline waters through the Florida Straits. The reduction in southward deep-water transport in CMIP6 is linked to a lack of INADW formed in the Nordic Seas flowing out over the Greenland–Iceland–Scotland Ridge into the northern Atlantic (Heuzé, 2021), and the reduction in the northward flow of upper waters is linked to a decrease in diffusive upwelling in the Indo-Pacific, which is related to increased stratification due to global warming (Li et al., 2020; Baker et al., 2023). The ability of coupled climate models to realistically include the critical processes of deep-water formation, mixing in ridge overflows and mid-ocean diffusive upwelling for future projections of ocean circulation should be carefully assessed. In particular, the representation of deep-water formation in coupled climate models could be examined in comparison with the observed production of deep water. Implementing mixing parameterizations for overflows (Holt et al., 2017) in coupled climate models could be assessed for its effectiveness in enabling the southward transport of INADW into and through the North Atlantic. Moreover, coupled climate models could be examined for their parameterizations of diffusive mixing and upwelling, testing how different parameterizations affect the global ocean overturning circulation over century timescales.

In terms of observations, our results suggest that the ongoing RAPID project should separately measure the Antilles Current and add it to the Florida Straits transport for a true measure of western boundary current transport for

comparison with modelled transport components. Furthermore, the Antilles Current transport should be separated from the net mid-ocean southward flow across 26° N in the upper 800 m that RAPID labels as thermocline recirculation so as to identify the actual mid-ocean thermocline recirculation associated with the wind stress curl. By separately estimating the Antilles Current transport contribution, the RAPID project could then provide well-defined estimates for the wind-driven and thermohaline contributions to the AMOC at 26° N.

Code availability. The code used to obtain the results of this study and a file containing metadata regarding the models are freely available on GitHub at https://github.com/jordibeunk/MSc_Thesis.git (Beunk, 2022).

Data availability. RAPID data and notes are freely available at https://rapid.ac.uk/rapidmoc/rapid_data/datadl.php (last access: May 2022). A total of 19 CMIP6 models are used. CMIP6 data were accessed and analysed using the JASMIN super-data-cluster (Lawrence et al., 2013). The choice of these models is motivated by the fact that both historical (2004–2015) data and future (2015–2100) projections under Shared Socioeconomic Pathway 5-8.5 are available for all variables used. The model data have been accessed through the Centre for Environmental Data Analysis (CEDA) archive at <https://data.ceda.ac.uk> (last access: May 2022).

Author contributions. This work is based on an MSc thesis by JB at the University of Utrecht (Beunk, 2022). JM, SD and HB designed the Master's project. SD and WH identified the student and supervised the project in Utrecht, while JM and HB provided advice during the project and write-up of the thesis. After finishing the thesis, JB initially indicated that he did not wish to write up the results for publication. HB prepared a draft for this paper based on JB's thesis. SD, WH and JM then edited the draft, and all authors added elements of discussion related to recent papers based on results from CMIP6. JB at a late stage indicated that he would like to participate in publishing this work, and all authors contributed to revising the work in response to referee comments.

Competing interests. The contact author has declared that none of the authors has any competing interests.

Disclaimer. Publisher's note: Copernicus Publications remains neutral with regard to jurisdictional claims made in the text, published maps, institutional affiliations, or any other geographical representation in this paper. While Copernicus Publications makes every effort to include appropriate place names, the final responsibility lies with the authors.

Acknowledgements. The UK Natural Environment Research Council, US National Science Foundation, and US National Oceanic and

Atmospheric Administration provide funding for the RAPID project and make the data freely available. We acknowledge the World Climate Research Programme, which, through its Working Group on Coupled Modelling, coordinated and promoted CMIP6. We thank the climate modelling groups for producing and making available their model outputs, the Earth System Grid Federation (ESGF) for archiving the data and providing access, and the multiple funding agencies which support CMIP6 and the ESGF. Harry Bryden was a lead investigator for the NERC-funded project that first deployed the transoceanic RAPID instrument array in 2004 under grant no. NER/T/S/2002/00481, and he has continued to carry out analyses involving the ongoing RAPID observations following formal retirement in 2011. Sybren Drijfhout and Jennifer Mecking have been funded by NERC through the project “Wider impacts of Subpolar North Atlantic decadal variability on the ocean and atmosphere (WISHBONE)” (grant no. NE/T0133478/1).

Financial support. This research has been supported by the UK Natural Environment Research Council (grant nos. NER/T/S/2002/00481 and NE/T0133478/1).

Review statement. This paper was edited by Agnieszka Beszczynska-Möller and reviewed by three anonymous referees.

References

- Asbjørnsen, H. and Årthun, M.: Deconstructing future AMOC decline at 26.5° N, *Geophys. Res. Lett.*, 50, e2023GL103515, <https://doi.org/10.1029/2023GL103515>, 2023.
- Baker, J. S., Bell, M. J., Jackson, L. C., Renshaw, R., Vallis, G. K., Watson, A. J. and Wood, R. A.: Overturning pathways control AMOC weakening in CMIP6 Models, *Geophys. Res. Lett.*, 50, e2023GL103381, <https://doi.org/10.1029/2023GL103381>, 2023.
- Beunk, J.: Comparing observed and modeled decomposition of the Atlantic Meridional Overturning Circulation at 26° N, MSc Thesis, Department of Geosciences, Utrecht University [code], 54 pp., <https://studenttheses.uu.nl/handle/20.500.12932/41572> (last access: 15 April 2024), 2022.
- Boucher, O., Denvil, S., Levavasseur, G., Cozic, A., Caubel, A., Foujols, M.-A., Meurdesoif, Y., Cadule, P., Devilliers, M., Dupont, E., and Lurton, T.: IPSL IPSL-CM6A-LR model output prepared for CMIP6 Scenario MIP SSP5-8.5, Version 20211003, Earth System Grid Federation, <https://doi.org/10.22033/ESGF/CMIP6.5271>, 2019.
- Boucher, O., Denvil, S., Levavasseur, G., Cozic, A., Caubel, A., Foujols, M.-A., Meurdesoif, Y., Balkanski, Y., Checa-Garcia, R., Hauglustaine, D., Bekki, S., and Marchand, M.: IPSL IPSL-CM6A-LR-INCA model output prepared for CMIP6 CMIP Historical, Version 20211003, Earth System Grid Federation, <https://doi.org/10.22033/ESGF/CMIP6.13601>, 2021.
- Bryden, H. L.: Wind-driven and buoyancy-driven circulation in the subtropical North Atlantic Ocean, *Proc. Roy. Soc. A*, 477, 20210172, <https://doi.org/10.1098/rspa.2021.0172>, 2021.
- Cao, J.: NUIST NESMv3 model output prepared for CMIP6 ScenarioMIP SSP5-8.5, Version 20211003, Earth System Grid Federation, <https://doi.org/10.22033/ESGF/CMIP6.8790>, 2019.
- Cao, J. and Wang, B.: NUIST NESMv3 model output prepared for CMIP6 CMIP historical, Version 20211003, Earth System Grid Federation, <https://doi.org/10.22033/ESGF/CMIP6.8769>, 2019.
- Chai, Z.: CAS CAS-ESM1.0 model output prepared for CMIP6 CMIP historical, Version 20211003, Earth System Grid Federation, <https://doi.org/10.22033/ESGF/CMIP6.3353>, 2020.
- Danabasoglu, G.: NCAR CESM2-WACCM model output prepared for CMIP6 ScenarioMIP SSP5-8.5, Version 20211003, Earth System Grid Federation, <https://doi.org/10.22033/ESGF/CMIP6.10115>, 2019a.
- Danabasoglu, G.: NCAR CESM2-WACCM-FV2 model output prepared for CMIP6 CMIP Historical, Version 20211003, Earth System Grid Federation, <https://doi.org/10.22033/ESGF/CMIP6.11298>, 2019b.
- DiNezio, P. N., Gramer, L. J., Johns, W. E., Meinen, C. S., and Baringer, M. O.: Observed interannual variability of the Florida Current: Wind forcing and the North Atlantic Oscillation, *J. Phys. Oceanogr.*, 39, 721–736, 2009.
- Ditlevsen, P. and Ditlevsen, S.: Warning of a forthcoming collapse of the Atlantic meridional overturning circulation, *Nat. Comm.*, 14, 4254, <https://doi.org/10.1038/s41467-023-39810-w>, 2023.
- EC-Earth Consortium (EC-Earth): EC-Earth-Consortium EC-Earth3 model output prepared for CMIP6 ScenarioMIP SSP5-8.5, Version 20211003, Earth System Grid Federation, <https://doi.org/10.22033/ESGF/CMIP6.4912>, 2019.
- EC-Earth Consortium (EC-Earth): EC-Earth-Consortium EC-Earth-3-CC model output prepared for CMIP6 CMIP historical, Version 20211003, Earth System Grid Federation, <https://doi.org/10.22033/ESGF/CMIP6.4702>, 2021.
- Eyring, V., Bony, S., Meehl, G. A., Senior, C. A., Stevens, B., Stouffer, R. J., and Taylor, K. E.: Overview of the Coupled Model Intercomparison Project Phase 6 (CMIP6) experimental design and organization, *Geosci. Model Dev.*, 9, 1937–1958, <https://doi.org/10.5194/gmd-9-1937-2016>, 2016.
- Good, P.: MOHC HadGEM3-GC31-LL model output prepared for CMIP6 ScenarioMIP SSP5-8.5, Version 20211003, Earth System Grid Federation, <https://doi.org/10.22033/ESGF/CMIP6.10901>, 2020.
- Good, P., Sellar, A., Tang, Y., Rumbold, S., Ellis, R., Kelley, D., and Kuhlbrodt, T.: MOHC UKESM1.0-LL model output prepared for CMIP6 ScenarioMIP SSP5-8.5, Version 20211003, Earth System Grid Federation, <https://doi.org/10.22033/ESGF/CMIP6.6405>, 2019.
- Heuzé, C.: Antarctic Bottom Water and North Atlantic Deep Water in CMIP6 models, *Ocean Sci.*, 17, 59–90, <https://doi.org/10.5194/os-17-59-2021>, 2021.
- Holt, J., Hyder, P., Ashworth, M., Harle, J., Hewitt, H. T., Liu, H., New, A. L., Pickles, S., Porter, A., Popova, E., Allen, J. I., Sidorn, J., and Wood, R.: Prospects for improving the representation of coastal and shelf seas in global ocean models, *Geosci. Model Dev.*, 10, 499–523, <https://doi.org/10.5194/gmd-10-499-2017>, 2017.
- Huang, W.: THU CIESM model output prepared for CMIP6 CMIP historical, Version 20211003, Earth System Grid Federation, <https://doi.org/10.22033/ESGF/CMIP6.8843>, 2019.

- Huang, W.: THU CIESM model output prepared for CMIP6 ScenarioMIP SSP5-8.5, Version 20211003, Earth System Grid Federation, <https://doi.org/10.22033/ESGF/CMIP6.8863>, 2020.
- Johns, W. E., Baringer, M. O., Beal, L. M., Cunningham, S. A., Kanzow, T., Bryden, H. L., Hirschi, J., Marotzke, J., Meinen, C., Shaw, B., and Curry, R.: Continuous, array-based estimates of Atlantic Ocean heat transport at 26.5°N, *J. Clim.*, 24, 2429–2449, <https://doi.org/10.1175/2010JCLI3997.1>, 2011.
- Johns, W. E., Elipot, S., Smeed, D. A., Moat, B., King, B., Volkov, D. L., and Smith, R. H.: Towards two decades of Atlantic Ocean mass and heat transports at 26.5°N, *Philos. T. R. Soc. A*, 381, 20220188, <https://doi.org/10.1098/rsta.2022.0188>, 2023.
- Jungclaus, J., Bittner, M., Wieners, K.-H., Wachsmann, F., Schupfner, M., Legutke, S., Giorgetta, M., Reick, C., Gayler, V., Haak, H., de Vrese, P., Raddatz, T., Esch, M., Mauritsen, T., von Storch, J.-S., Behrens, J., Brovkin, V., Claussen, M., Crueger, T., Fast, I., Fiedler, S., Hagemann, S., Hohenegger, C., Jahns, T., Kloster, S., Kinne, S., Lasslop, G., Kornblueh, L., Marotzke, J., Matei, D., Meraner, K., Mikolajewicz, U., Modali, K., Müller, W., Nabel, J., Notz, D., Peters-von Gehlen, K., Pincus, R., Pohlmann, H., Pongratz, J., Rast, S., Schmidt, H., Schnur, R., Schulzweida, U., Six, K., Stevens, B., Voigt, A., and Roeckner, E.: MPI-M MPI-ESM1.2-HR model output prepared for CMIP6 CMIP historical, Version 20211003, Earth System Grid Federation, <https://doi.org/10.22033/ESGF/CMIP6.6594>, 2019.
- Lawrence, B. N., Bennett, V. L., Churchill, J., Juckes, M., Kershaw, P., Pascoe, S., Pepler, S., Pritchard, M., and Stephens, A.: Storing and manipulating environmental big data with JASMIN, in: 2013 IEEE International Conference on Big Data [data set], 6–9 October 2013, Silicon Valley, CA, USA, 68–75, <https://doi.org/10.1109/BigData.2013.6691556>, 2013.
- Lee, J.-Y., J. Marotzke, J., Bala, G., Cao, L., Corti, S., Dunne, J.P., Engelbrecht, F., Fischer, E., Fyfe, J.C., Jones, C., Maycock, A., Mutemi, J., Ndiaye, O., Panickal, S., and Zhou, T.: Future Global Climate: Scenario-Based Projections and Near-Term Information, in: *Climate Change 2021: The Physical Science Basis. Contribution of Working Group I to the Sixth Assessment Report of the Intergovernmental Panel on Climate Change*, edited by: Masson-Delmotte, V., Zhai, P., Pirani, A., Connors, S.L., Péan, C., Berger, S., Caud, N., Chen, Y., Goldfarb, L., Gomis, M. I., Huang, M., Leitzell, K., Lonnoy, E., Matthews, J. B. R., Maycock, T. K., Waterfield, T., Yelekçi, O., Yu, R., and Zhou, B., Cambridge University Press, Cambridge, United Kingdom and New York, NY, USA, 553–672, <https://doi.org/10.1017/9781009157896.006>, 2021.
- Levang, S. J. and Schmitt, R. W.: What Causes the AMOC to Weaken in CMIP5?, *J. Clim.*, 33, 1535–1545, 2020.
- Li, G., Cheng, L., Zhu, J., Trenberth, K. E., Mann, M. E., and Abraham, J. P.: Increasing ocean stratification over the past half-century, *Nat. Clim. Change*, 10, 1116–1123, 2020.
- Lovato, T. and Peano, D.: CMCC CMCC-CM2-SR5 model output prepared for CMIP6, CMIP historical, Version 20211003, Earth System Grid Federation, <https://doi.org/10.22033/ESGF/CMIP6.3825>, 2020a.
- Lovato, T. and Peano, D.: CMCC CMCC-CM2-SR5 model output prepared for CMIP6, ScenarioMIP SSP5-8.5, Version 20211003, Earth System Grid Federation, <https://doi.org/10.22033/ESGF/CMIP6.3896>, 2020b.
- Lovato, T., Peano, D., and Butenschön, M.: CMCC CMCC-ESM2 model output prepared for CMIP6 CMIP historical, Version 20211003, Earth System Grid Federation, <https://doi.org/10.22033/ESGF/CMIP6.13195>, 2021a.
- Lovato, T., Peano, D., and Butenschön, M.: CMCC CMCC-ESM2 model output prepared for CMIP6 ScenarioMIP SSP5-8.5, Version 20211003, Earth System Grid Federation, <https://doi.org/10.22033/ESGF/CMIP6.13259>, 2021b.
- McCarthy, G. D. and Caesar, L.: Can we trust projections of AMOC weakening based on climate models that cannot reproduce the past?, *Philos. T. R. Soc.*, 381, 2262, <https://doi.org/10.1098/rsta.2022.0193>, 2023.
- Mecking, J. V. and Drijfhout, S. S.: The decrease in ocean heat transport in response to global warming, *Nat. Clim. Change*, 13, 1229–1236, <https://doi.org/10.1038/s41558-023-01829-8>, 2023.
- Meinen, C. S., Johns, W. E., Moat, B. I., Smith, R. H., Johns, E. M., Rayner, D., Frajka-Williams, E., Garcia, R. F., and Garzoli, S. L.: Structure and variability of the Antilles Current at 26.5°N, *J. Geophys. Res.-Ocean.*, 124, 3700–3723, <https://doi.org/10.1029/2018JC014836>, 2019.
- Moat, B. I., Smeed, D. A., Frajka-Williams, E., Desbruyères, D. G., Beaulieu, C., Johns, W. E., Rayner, D., Sanchez-Franks, A., Baringer, M. O., Volkov, D., Jackson, L. C., and Bryden, H. L.: Pending recovery in the strength of the meridional overturning circulation at 26°N, *Ocean Sci.*, 16, 863–874, <https://doi.org/10.5194/os-16-863-2020>, 2020.
- Moat, B. I., Frajka-Williams, E., Smeed, D. A., Rayner, D., Johns, W. E., Baringer, M. O., Volkov, D. L., and Collins, J.: Atlantic meridional overturning circulation observed by the RAPID-MOCHA-WBTS (RAPID-meridional Overturning Circulation and Heatflux Array-Western Boundary Time Series) array at 26°N from 2004 to 2020 (v2020.2), British Oceanographic Data Centre, Natural Environment Research Council [data set], <https://doi.org/10.5285/e91b10af-6f0a-7fa7-e053-6c86abc05a09>, 2022.
- Munk, W.: Abyssal recipes, *Deep-Sea Res.*, 13, 707–730, 1966.
- O'Neill, B. C., Tebaldi, C., van Vuuren, D. P., Eyring, V., Friedlingstein, P., Hurtt, G., Knutti, R., Kriegler, E., Lamarque, J.-F., Lowe, J., Meehl, G. A., Moss, R., Riahi, K., and Sanderson, B. M.: The Scenario Model Intercomparison Project (ScenarioMIP) for CMIP6, *Geosci. Model Dev.*, 9, 3461–3482, <https://doi.org/10.5194/gmd-9-3461-2016>, 2016.
- Piecuch, C. G. and Beal, L. M.: Robust Weakening of the Gulf Stream During the Past Four Decades Observed in the Florida Straits, *Geophys. Res. Lett.*, 50, e2023GL105170, <https://doi.org/10.1029/2023gl105170>, 2023.
- Ridley, J., Menary, M., Kuhlbrodt, T., Andrews, M., and Andrews, T.: MOHCHadGEM3-GC31-LL model output prepared for CMIP6 CMIP historical, Version 20211003, Earth System Grid Federation, <https://doi.org/10.22033/ESGF/CMIP6.6109>, 2019a.
- Ridley, J., Menary, M., Kuhlbrodt, T., Andrews, M., and Andrews, T.: MOHCHadGEM3-GC31-MM model output prepared for CMIP6 CMIP historical, Version 20211003, Earth System Grid Federation, <https://doi.org/10.22033/ESGF/CMIP6.6112>, 2019b.
- Roberts, M. J., Jackson, L. C., Roberts, C. D., Meccia, V., Docquier, D., Koenigk, T., Ortega, P., Moreno-Chamarro, E., Bellucci, A., Coward, A., Drijfhout, S., Exarchou, E., Gutjahr, O., Hewitt, H., Iovino, D., Lohmann, K., Putrasahan, D., Schiemann,

- R., Seddon, J., Terray, L., Xu, X., Zhang, Q., Chang, P., Yeager, S. G., Castruccio, F. S., Zhang, S., and Wu, L.: Sensitivity of the Atlantic meridional overturning circulation to model resolution in CMIP6 HighResMIP simulations and implications for future changes, *J. Adv. Model. Earth Syst.*, 12, e2019MS002014, <https://doi.org/10.1029/2019MS002014>, 2020.
- Rong, X.: CAMS CAMS-CSM1.0 model output prepared for CMIP6 CMIP historical, Version 20211003, Earth System Grid Federation, <https://doi.org/10.22033/ESGF/CMIP6.9754>, 2019a.
- Rong, X.: CAMS CAMS-CSM1.0 model output prepared for CMIP6 ScenarioMIP SSP5-8.5, Version 20211003, Earth System Grid Federation, <https://doi.org/10.22033/ESGF/CMIP6.11052>, 2019b.
- Schupfner, M., Wieners, K.-H., Wachsmann, F., Steger, C., Bittner, M., Jungclaus, J., Früh, B., Pankatz, K., Giorgetta, M., Reick, C., Legutke, S., Esch, M., Gayler, V., Haak, H., de Vrese, P., Raddatz, T., Mauritsen, T., von Storch, J.-S., Behrens, J., Brovkin, V., Claussen, M., Crueger, T., Faust, I., Fiedler, S., Hagemann, S., Hohenegger, C., Jahns, T., Kloster, S., Kinne, S., Lasslop, G., Kornblueh, L., Marotzke, J., Matei, D., Meraner, K., Mikolajewicz, U., Modali, K., Müller, W., Nabel, J., Notz, D., Peters-von Gehlen, K., Pincus, R., Pohlmann, H., Pongratz, J., Rast, S., Schmidt, H., Schnur, R., Schulzweida, U., Six, K., Stevens, B., Voigt, A., and Roeckner, E.: DKRZ MPI-ESM1.2-HR model output prepared for CMIP6 ScenarioMIPssp585, Version 20211003, Earth System Grid Federation, <https://doi.org/10.22033/ESGF/CMIP6.4403>, 2019.
- Seferian, R.: CNRM-CERFACS CNRM-ESM2-1 model output prepared for CMIP6 CMIP Historical, Version 20211003, Earth System Grid Federation, <https://doi.org/10.22033/ESGF/CMIP6.4068>, 2018.
- Smeed, D. A., Josey, S. A., Beaulieu, C., Johns, W.E., Moat, B. I., Frajka-Williams, E., Rayner, D., Meinen, C. S., Baringer, M. O., Bryden, H. L., and McCarthy, G. D.: The North Atlantic Ocean is in a state of reduced overturning, *Geophys. Res. Lett.*, 45, 1527–1533, <https://doi.org/10.1002/2017GL076350>, 2018.
- Song, Z., Qiao, F., Bao, Y., Shu, Q., Song, Y., and Yang, X.: FIO-QLNM FIO-ESM2.0 model output prepared for CMIP6 CMIP historical, Version 20211003, Earth System Grid Federation, <https://doi.org/10.22033/ESGF/CMIP6.9199>, 2019a.
- Song, Z., Qiao, F., Bao, Y., Shu, Q., Song, Y., and Yang, X.: FIO-QLNM FIO-ESM2.0 model output prepared for CMIP6 ScenarioMIP SSP5-8.5, Version 20211003, Earth System Grid Federation, <https://doi.org/10.22033/ESGF/CMIP6.9214>, 2019b.
- Stommel, H.: The westward intensification of wind-driven ocean currents, *Eos, Trans. Am. Geophys. Union*, 29, 202–206, 1948.
- Swart, N. C., Cole, J. N. S., Kharin, V. V., Lazare, M., Scinocca, J. F., Gillett, N. P., Anstey, J., Arora, V., Christian, J. R., Jiao, Y., Lee, W. G., Majaess, F., Saenko, O. A., Seiler, C., Seinen, C., Shao, A., Solheim, L., von Salzen, K., Yang, D., Winter, B., and Sigmund, M.: CCCma CanESM5 model output prepared for CMIP6 CMIP historical, Version 20211003, Earth System Grid Federation, <https://doi.org/10.22033/ESGF/CMIP6.3610>, 2019a.
- Swart, N. C., Cole, J. N. S., Kharin, V. V., Lazare, M., Scinocca, J. F., Gillett, N. P., Anstey, J., Arora, V., Christian, J. R., Jiao, Y., Lee, W. G., Majaess, F., Saenko, O. A., Seiler, C., Seinen, C., Shao, A., Solheim, L., von Salzen, K., Yang, D., Winter, B., and Sigmund, M.: CCCma CanESM5 model output prepared for CMIP6 ScenarioMIP SSP5-8.5, Version 20211003, Earth System Grid Federation, <https://doi.org/10.22033/ESGF/CMIP6.3696>, 2019b.
- Tang, Y., Rumbold, S., Ellis, R., Kelley, D., Mulcahy, J., Seljar, A., Walton, J., and Jones, C.: MOHC UKESM1.0-LL model output prepared for CMIP6 CMIP Historical, Version 20211003 Earth System Grid Federation, <https://doi.org/10.22033/ESGF/CMIP6.6113>, 2019.
- Toggweiler, J. R. and Samuels, B.: On the ocean's large-scale circulation near the limit of no vertical mixing, *J. Phys. Oceanogr.*, 28, 1832–1852, [https://doi.org/10.1175/1520-0485\(1998\)028<1832:OTOSLS>2.0.CO;2](https://doi.org/10.1175/1520-0485(1998)028<1832:OTOSLS>2.0.CO;2), 1998.
- Unknown: CAS CAS-ESM1.0 model output prepared for CMIP6 ScenarioMIP SSP5-8.5, Earth System Grid Federation, <http://cera-www.dkrz.de/WDCC/meta/CMIP6/CMIP6.ScenarioMIP.CAS.CAS-ESM2-0.SSP5-8.5> (last access: 15 May 2022), 2018.
- Voltaire, A.: CNRM-CERFACS CNRM-CM6-1-HR model output prepared for CMIP6 CMIP Historical, Version 20211003, Earth System Grid Federation, <https://doi.org/10.22033/ESGF/CMIP6.4067>, 2019a.
- Voltaire, A.: CNRM-CERFACS CNRM-CM6-1-HR model output prepared for CMIP6 ScenarioMIP SSP5-8.5, Version 20211003, Earth System Grid Federation, <https://doi.org/10.22033/ESGF/CMIP6.4225>, 2019b.
- Weijer, W., Cheng, W., Garuba, O. A., Hu, A., and Nadiga, B. T.: CMIP6 models predict significant 21st century decline of the Atlantic Meridional Overturning Circulation, *Geophys. Res. Lett.*, 47, e2019GL086075, <https://doi.org/10.1029/2019GL086075>, 2020.
- Wieners, K.-H., Giorgetta, M., Jungclaus, J., Reick, C., Esch, M., Bittner, M., Legutke, S., Schupfner, M., Wachsmann, F., Gayler, V., Haak, H., de Vrese, P., Raddatz, T., Mauritsen, T., von Storch, J.-S., Behrens, J., Brovkin, V., Claussen, M., Crueger, T., Fast, I., Fiedler, S., Hagemann, S., Hohenegger, C., Jahns, T., Kloster, S., Kinne, S., Lasslop, G., Kornblueh, L., Marotzke, J., Matei, D., Meraner, K., Mikolajewicz, U., Modali, K., Müller, W., Nabel, J., Notz, D., Peters-von Gehlen, K., Pincus, R., Pohlmann, H., Pongratz, J., Rast, S., Schmidt, H.; Schnur, R., Schulzweida, U., Six, K., Stevens, B., Voigt, A., and Roeckner, E.: MPI-M MPI-ESM1.2-LR model output prepared for CMIP6 CMIP historical, Version 20211003, Earth System Grid Federation, <https://doi.org/10.22033/ESGF/CMIP6.6595>, 2019a.
- Wieners, K.-H., Giorgetta, M., Jungclaus, J., Reick, C., Esch, M., Bittner, M., Gayler, V., Haak, H., de Vrese, P., Raddatz, T., Mauritsen, T., von Storch, J.-S., Behrens, J., Brovkin, V., Claussen, M., Crueger, T., Fast, I., Fiedler, S., Hagemann, S., Hohenegger, C., Jahns, T., Kloster, S., Kinne, S., Lasslop, G., Kornblueh, L., Marotzke, J., Matei, D., Meraner, K., Mikolajewicz, U., Modali, K., Müller, W., Nabel, J., Notz, D., Peters-von Gehlen, K., Pincus, R., Pohlmann, H., Pongratz, J., Rast, S., Schmidt, H., Schnur, R., Schulzweida, U., Six, K., Stevens, B., Voigt, A., and Roeckner, E.: MPI-M MPI-ESM1.2-LR model output prepared for CMIP6 ScenarioMIP SSP5-8.5, Version 20211003, Earth System Grid Federation, <https://doi.org/10.22033/ESGF/CMIP6.6705>, 2019b.
- Yukimoto, S., Koshiro, T., Kawai, H., Oshima, N., Yoshida, K., Urakawa, S., Tsujino, H., Deushi, M., Tanaka, T., Hosaka, M., Yoshimura, H., Shindo, E., Mizuta, R., Ishii, M., Obata, A., and Adachi, Y.: MRI MRI-ESM2.0 model output prepared for

- CMIP6 CMIP historical, Version 20211003, Earth System Grid Federation, <https://doi.org/10.22033/ESGF/CMIP6.6842>, 2019a.
- Yukimoto, S., Koshiro, T., Kawai, H., Oshima, N., Yoshida, K., Urakawa, S., Tsujino, H., Deushi, M., Tanaka, T., Hosaka, M., Yoshimura, H., Shindo, E., Mizuta, R., Ishii, M., Obata, A., and Adachi, Y.: MRI MRI-ESM2.0 model output prepared for CMIP6 ScenarioMIP SSP5-8.5, Version 20211003, Earth System Grid Federation, <https://doi.org/10.22033/ESGF/CMIP6.6929>, 2019b.
- Zhao, J. and Johns, W.: Wind-forced interannual variability of the Atlantic Meridional Overturning Circulation at 26.5°N, *J. Geophys. Res.-Ocean.*, 119, 2403–2419, <https://doi.org/10.1002/2013JC009407>, 2014.